ORIGINAL RESEARCH

Clinical significance of miR-34a expression in thyroid diseases – an ^{18}F-FDG PET-CT study

Long Chen[1,*]
Conghui Yang[1,*]
Jun Feng[2,*]
Xin Liu[3,*]
Yadong Tian[1]
Lei Zhao[1]
Ran Xie[1]
Chao Liu[4]
Sheng Zhao[1]
Hua Sun[1]

[1]Department of PET/CT Center,
[2]Department of Radiology,
[3]Department of Pathology,
[4]Department of Nuclear Medicine,
Yunnan Tumor Hospital, The Third
Affiliated Hospital of Kunming Medical
University, Kunming, People's Republic
of China

*These authors contributed equally to
this work

Purpose: To evaluate the possible roles of miR-34a expression in thyroid lesions, to unravel the correlation between fluorodeoxyglucose (FDG) uptake and miR-34a expression and moreover, to discover the underlying mechanisms by which miR-34a regulates FDG avidity.

Methods: We retrospectively reviewed 75 patients with pathology-confirmed thyroid diseases who underwent ^{18}F-FDG positron emission tomography/computed tomography (PET/CT) within 3 months before undergoing thyroid surgery and miR-34a analysis from June 2012 to July 2017. ^{18}F-FDG uptake of thyroid lesions was also analyzed semiquantitatively using maximum standardized uptake value (SUVmax). The association between miR-34a expression and clinicopathological variables (age, sex, TNM stage, histopathology, lesion numbers, location and ^{18}F-FDG avidity) was investigated. When there were multiple lesions in thyroid bed, only the one with the highest ^{18}F-FDG uptake was analyzed. Next, we inhibited the miR-34a expression in TPC-1 cells and detected the expression of glucose transporter 1 (GLUT1) mRNA and protein.

Results: In the patients cohort, miR-34a was upregulated in those with malignant thyroid diseases compared with benign lesions. The expression of miR-34a was associated with tumor stages, histopathological types and SUVmax. There was an inverse relationship between miR-34a expression and SUVmax in patients with thyroid diseases (Spearman correlation coefficient = –0.553, $P < 0.0001$). With an SUVmax of 4.3 as the threshold, sensitivity and specificity of the prediction of miR-34a expression (low or high) were 70% and 94.3%, respectively. The area under the receiver operating characteristic curve was 0.843 (95% confidence interval: 0.749, 0.936; $P = 0.001$). Inhibiting miR-34a in TPC-1 cells significantly increased GLUT1 mRNA and protein expression.

Conclusion: miR-34a expression was upregulated in thyroid lesions, negatively correlated with SUVmax and can be predicted by FDG SUVmax. In addition, miR-34a may regulate FDG avidity via targeting GLUT1.

Keywords: miR-34a, thyroid cancer, PET/CT

Introduction

Thyroid lesions are one of the most common endocrine-related diseases worldwide. The types of thyroid tumors include benign adenoma and malignant papillary thyroid carcinoma (PTC), follicular thyroid carcinoma (FTC), medullary thyroid carcinoma (MTC) and anaplastic thyroid carcinoma (ATC). PTC, which is relatively less harmful compared to other cancers, is the most common type of thyroid carcinoma, contributing to 80% of all thyroid malignancies, with an overall 10-year survival rate of more than 90%.[1] However, a significant increase in annual incidence is observed for papillary

Correspondence: Sheng Zhao; Hua Sun
Department of PET/CT Center, Yunnan
Tumor Hospital, The Third Affiliated
Hospital of Kunming Medical University,
Number 519 Kunzhou Road, Xishan,
Kunming 650118, Yunnan, People's
Republic of China
Email 943537426@qq.com; 649790827@
qq.com

carcinomas (from 6.7% to 10.3%) around the world, without statistically significant decrease in mortality.[2–5] Using ultrasonography (US) and US-guided fine-needle aspiration (FNA) biopsies, impalpable mini-sized thyroid disease could be detected easily.[6] Thyroid carcinoma is considered a curable disease; however, local recurrence and/or distant metastasis may occur in some patients, which indicates that accurate diagnosis and appropriate risk evaluation are still necessary. US-guided FNA biopsy has been thought to be the gold standard for thyroid nodule diagnosis, with correct final diagnoses in 70%–80% of cases, leaving 20%–30% of cases ambiguous.[7] New biomarkers which may change clinical outcomes, including operative strategy and prognosis, remain to be discovered.

MicroRNAs (miRNAs), which were firstly identified in *Caenorhabditis elegans*, are noncoding, endogenous small RNA molecules containing 18–23 nucleotides and regulate gene expression by binding to the 3′-UTR of specific "target" mRNA.[8] By regulating the expression of specific target mRNAs at the posttranscriptional level, miRNAs act as oncogenes as well as tumor suppressors. Recent studies have shown that miR-34a is involved in numerous biological processes, especially in cancers (Table 1).

miR-34 is a key regulator of tumor development, and miR-34a, miR-34b and miR-34c are the major members of the miR-34 precursor family. miR-34a has been reported to be upregulated in PTC tissues and cell lines.[25,26] However, no research has thoroughly elucidated the relationship between miR-34a and clinical characteristics so far.

Glucose metabolism can be molecularly imaged in vivo with ^{18}F-fluorodeoxyglucose positron emission tomography (^{18}F-FDG PET), and the uptake of FDG has been correlated with tumor proliferation in thyroid carcinomas. FDG PET scans are gaining an important role in thyroid cancer for

Table 1 Overview of miR-34a roles in cancers

Cancer type	miR-34a significance	Authors	Reference
Breast carcinoma	Met oncogene is unaffected by miR-34a in nonmetastatic and metastatic breast carcinomas, while in bone metastasis miR-34a correlates with Met, a key player of the bone-metastatic process, expression	Maroni et al	9
Head and neck squamous cell carcinoma	Forced miR-34a expression induced cell cycle arrest and senescence; genes, including FUT1, AXL and MAP2K1 were identified as the novel targets of miR-34a by qPCR and luciferase assay	Wang et al	10
Ovarian	Levels of miR-34a are downregulated in ovarian cancer patients. Introduction of miR-34a in ovarian cancer 94 cells resulted in reduced proliferation, motility and invasion		
Gastric cancer	Silencing miR-34a activates IGF2BP3, which ranked number 1 of the upregulated genes and associated with poor disease-specific survival	Zhou et al	11
Osteosarcoma	miR-34a targets DLL1, leading to the ATF2/ATF3/ATF4 signaling pathway, significantly altering and negatively regulating the multi-chemoresistance of osteosarcoma	Pu et al	12
	miR-34a inhibits growth and metastasis of osteosarcoma cells both in vitro and in vivo through targeting c-Met	Yan et al	13
Myeloma	Therapeutic potential of synthetic miR-34a against human multiple myeloma was shown partially by repressing BCL-2 and CDK6	Di Martino et al	14
Hepatocellular carcinoma	miR-34a, by mimicking ST3GAL5, significantly changes HCC malignant behaviors and oncogenicity in in vitro and in vivo assays, acting as tumor suppressor	Cai et al	15
	miR-34a may inhibit the proliferation of HCC cells and induce their apoptosis via regulating HDAC1 expression	Sun et al	16
Pancreatic cancer	miR-34a is downregulated in the majority of pancreatic cancers and inhibited the growth of MiaPaCa-2 subcutaneous xenografts	Pramanik et al	17
Melanoma	Overexpression of miR-34a decreased the invasiveness of melanoma cells, partially involved in P53	Yamazaki et al	18
Colorectal cancer	miR-34a mediates OXA resistance of CRC by inhibiting macroautophagy via TGF-β/Smad4 pathway	Sun et al	19
Lung cancer	Hypermethylation of miR-34a promoter was detected in 68.7% lung adenocarcinoma	Daugaard et al	20
Leukemia	miR-34a promoted cell apoptosis and inhibited autophagy by targeting HMGB1 in acute myeloid leukemia	Liu et al	21
Renal cell cancer	miR-34a was upregulated in 198 RCC patients and correlated positively with HNF4A	Fritz et al	22
Cervical cancer	Forced expression of miR-34a inhibited proliferation, migration and invasion by reducing HMGB1 mRNA and protein levels	Chandrasekaran et al	23
Prostate cancer	Involved in chemoresistance and therapeutic efficacy of PTX in PTC-resistant prostate cancer	Wen et al	24

Abbreviations: HCC, hepatocellular carcinoma; OXA, oxaliplatin; CRC, colorectal cancer; RCC, renal cell carcinoma; PTX, paclitaxel; PTC, papillary thyroid carcinoma; qPCR, quantitative polymerase chain reaction.

initial staging, radiation therapy planning and restaging after therapy.[27–29] Furthermore, miR-34a was found to be significantly upregulated in type 2 diabetes,[30] indicating that miR-34a possibly regulates glycolysis, glucose metabolism and FDG avidity. Researches have revealed that glucose transporter 1 (GLUT1) plays crucial roles in transporting 18F-FDG into the cell by acting as a key rate-limiting enzyme.[31,32] Thus, quantification of glucose metabolism with FDG PET may present a noninvasive method to predict miR-34a expression. We retrospectively examined a cohort of patients with thyroid diseases who had underwent miR-34a expression testing and pretreatment FDG PET, and explored the clinical significance of miR-34a expression as well as the relationship between miR-34a expression and FDG avidity. The study flow chart is shown in Figure 1.

Materials and methods
Patients, human tissues and cell culture
This study was approved by the Institutional Review Board of the Third Affiliated Hospital of Kunming Medical University.
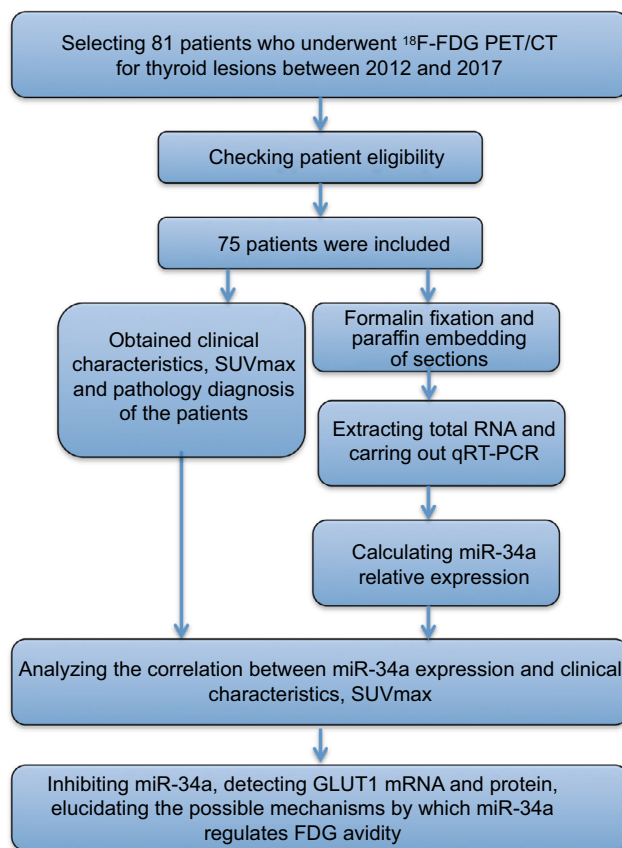

Figure 1 Study flowchart showing the inclusion and exclusion criteria and the entire study design.
Abbreviations: FDG, fluorodeoxyglucose; GLUT1, glucose transporter 1; PET/CT, positron emission tomography/computed tomography; qRT-PCR, quantitative reverse transcription-polymerase chain reaction; SUVmax, maximum standardized uptake value.

All patients whose tissue samples were used were informed about the study, and a written informed consent was obtained from them. Due to the retrospective design of this study, written informed patient consent for reviewing their medical records was waived by our institutional review board, but confidentiality of patient data was still confirmed. The records of patients with newly diagnosed thyroid diseases who underwent FDG PET/CT prior to thyroid surgery at our institution from June 2012 to July 2017 were reviewed. We identified a total of 81 patients with thyroid lesions who underwent FDG PET/CT within 1 month prior to operation. Of these patients, 6 with initial other primary cancers (4 had in lung and the other 2 in breast) were excluded. Ultimately, 75 patients were enrolled in this retrospective study, and the corresponding formalin-fixed paraffin-embedded (FFPE) surgical specimens were obtained from the Department of Pathology. Human TPC-1 cell line was purchased from Shanghai Cancer Institute (Shanghai, People's Republic of China). TPC-1 cells were maintained in Dulbecco's Modified Eagle's Medium supplemented with 10% fetal bovine serum (Thermo Fisher Scientific, Waltham, MA, USA) at 37°C with 5% CO_2 in a humidified incubator.

Clinicopathological data analysis
Medical records were reviewed to determine sex and age at diagnosis. Pathology reports were reviewed for the following data: tumor size, multifocality, histopathology and location. TNM stage was assigned based on the AJCC Cancer Staging Manual 8th edition.[33] None of the patients had a history of neck radiation. Thyroid cancer was diagnosed pathologically after surgery. Patients were divided into 2 groups according to miR-34a expression (0.36 is the average relative expression of miR-34a among all the patients). Basic information of the patients is shown in Table 2.

Interpretation and analysis of FDG PET/CT scan
18F-FDG PET/CT scans were obtained with an advanced integrated PET/CT scanner (Biograph 16; Siemens). All patients fasted for at least 6 h before FDG was intravenously injected in the resting state. A standard dose of 0.12 mCi·kg^{-1} 18F-FDG tracer was used for all patients. In the period between injection of 18F-FDG tracer and image acquisition, the patients were instructed to remain seated or recumbent and silent in order to minimize muscular 18F-FDG uptake. Patients were kept warm 30–60 min prior to tracer injection and throughout the uptake period in order to minimize 18F-FDG accumulation in brown fat. Blood glucose was measured in all diabetic

Table 2 miR-34a expression in thyroid lesions and clinical characteristics

Clinical characteristics	Patients (n)	miR34a expression (mean ± SD)	P
Age (years)			
≤45	41	0.3495 ± 0.02	0.2729
>45	34	0.3759 ± 0.01	
Gender			
Male	43	0.3551± 0.02	0.5398
Female	32	0.3700 ± 0.02	
Tumor stage			
I/II	47	0.4111 ± 0.01	<0.0001
III/IV	18	0.2811 ± 0.02	
Histopathology			
PTC	41	0.4251 ± 0.08	<0.0001
FTC	12	0.3217 ± 0.04	
MTC	8	0.3050 ± 0.05	
ATC	4	0.2650 ± 0.05	
Goiter	10	0.1980 ± 0.03	
Lesion numbers			
Single	51	0.3629 ± 0.02	0.4865
Multiple	24	0.3442 ± 0.02	
Location			
Left	38	0.3597 ± 0.11	0.8570
Right	26	0.3600 ± 0.11	
Both	11	0.3400 ± 0.12	
SUVmax			<0.0001
Low (≤3.63)	27	0.4326 ± 0.02	
High (>3.63)	48	0.3098 ± 0.01	

Abbreviations: SD, standard deviation; PTC; papillary thyroid carcinoma; FTC, follicular thyroid carcinoma; MTC, medullary thyroid carcinoma; ATC, anaplastic thyroid carcinoma; SUVmax, maximum standardized uptake value.

patients to ensure that it was within acceptable limits. Patients with blood glucose >10 mmol/L were rescheduled. PET/CT images were acquired 60 min after FDG injection with a Siemens scanner, with the patients positioned with both arms down. The CT scan comprised dual-slice CT. The scan field of view was from the skull base to the mid-thigh level. The CT scan was performed using a standardized protocol of 120 kV X-ray voltage, 50 mA tube current, a 0.75 s tube rotation time per rotation, 1.5 pitch and a section thickness of 5 mm. Immediately after the CT scan, PET images were acquired using a conventional 3-dimensional protocol with 2.5 min per frame. Two nuclear medicine physicians with more than 10 years experience assessed the FDG PET/CT images. Based on FDG uptake in thyroid, tumors were categorized: tumor with a focal discrete FDG uptake in the thyroid that corresponds to the location recorded in pathological reports was categorized as FDG-avid tumor, while tumor with no discernible FDG uptake higher than surrounding thyroid tissue was categorized as non-FDG-avid tumor. In the case of multifocal tumors, the largest tumor was

selected for interpretation. After the acquisition, maximum standardized uptake value (SUVmax) was assessed on the Siemens syngo MultiModality WorkPlace system by a single nuclear medicine physician. The SUVmax was defined as the decay-corrected radioactivity per unit volume divided by the injected radioactivity per body weight of the patient. SUVmax was determined by manually placing a cylindrical region of interest (ROI) over the basin of the primary tumor site. This was done on trans-axial images by an experienced nuclear medicine physician. ROIs were drawn to cover the whole tumor. In cases of multiple malignant nodules, an ROI was drawn on the largest one.

miR-34a inhibitor transfection

To assess the effect of miR-34a inhibitor on GLUT1 expression, we employed the miR-34a inhibitor (5′-ACAAC-CAGCUAAGACACUGCC A-3′) chemically synthesized by GenePharma (Shanghai, People's Republic of China) using Lipofectamine 2000 (Thermo Fisher Scientific) according to the manufacturer's protocol. The nonsense single-stranded RNA (5′-CAGUACUUUUGUGUAGUA CAA-3′), chemically synthesized by GenePharma, was transfected into the negative control (NC) group.

RNA extraction, reverse transcription and RT-qPCR

Twenty-micrometer sections were cut from FFPE surgical specimen of each patient. Macrodissection of specimens was performed to obtain at least 75% of tumor cells in samples before RNA extraction. Total RNA was isolated from tissue samples using RecoverAll™ total nucleic acid isolation kit for FFPE specimen (AM1975; Thermo Fisher Scientific) according to the manufacturer's instructions. Concentration and purity of total RNA was assessed by monitoring $A_{260/280}$ ratio and $A_{260/230}$ ratio using NanodropND-1000 (Thermo Fisher Scientific). $A_{260/280}$ ratios of 1.8–2.1 indicated acceptable RNA purity. The integrity of RNA was then analyzed using 1% agarose gel electrophoresis, and the gel was then stained using ethidium bromide. A total of 1 μg RNA was used to produce cDNA using a TaqMan miRNA reverse transcription kit according to the manufacturer's instructions (Thermo Fisher Scientific). Real-time PCR was carried out using SYBR green Real-time PCR Master Mix on an ABI 7500 Real-time PCR instrument (Applied Biosystems). The conditions of real-time PCR were as follows: 95°C for 30 s, 95°C for 5 s, 55°C for 10 s to anneal and 72°C for 15 s to elongate followed by 35 cycles. U6 was used as internal control. Relative gene expression levels were calculated

using the $2^{-\Delta\Delta Ct}$ method. The sequences of primers used for miR-34a expression analysis were as follows: forward, 5′-GTCCTCTAGACTAAGGGGTTGCCATGGTGT-3′; reverse, 5′-GTCCGGCCGGCCAGAGGCAATATA-CATTCTCCCGCA-3′.

Western blot analysis

Samples of 20 μg total protein were separated on 10% SDS-PAGE, and were transferred onto a polyvinylidene difluoride (PVDF) membrane (Bio-Rad, Hercules, CA, USA). The PVDF membrane was incubated with phosphate-buffered saline, containing 5% milk, overnight at 4°C. Subsequently, the PVDF membrane was incubated with monoclonal mouse anti-human GLUT1 and β-actin primary antibodies (1:2000 and 1:2500; Abcam) at room temperature for 4 h, respectively. This was followed by incubation with rabbit anti-mouse IgG-HRP (1:2000; Santa Cruz Biotechnology) at room temperature for 1 h. An enhanced chemiluminescence kit (Pierce Biotechnology) was then used to detect chemilumi-nescence. The relative protein expression was analyzed by Image-Pro Plus software (version 6.0; Media Cybernetics, Inc., Rockville, MD, USA), represented as the density ratio versus β-actin.

Statistical analysis

All statistical analyses were performed using IBM SPSS version 22 by 2 bio-statisticians. Univariate analysis of SUV-max was performed using univariate analysis. Patients' age, tumor and lymph node stage and, miR-34a expression were included as independent variables into the model. Spear-man rank correlation was used to determine the association between miR-34a expression and SUVmax. The receiver operating characteristic (ROC) curve was used to assess the best threshold of SUVmax which was used to predict miR-34a expression. The best threshold of SUVmax was based on the highest Youden index. The miR-34a expression and SUVmax of thyroid lesions were evaluated for calculating the area under the ROC curve and Youden index for determining the cutoff value for SUV_{max}. The Youden index, which is a comprehensive measurement for the performance of a diagnostic test, was generated considering every possible cutoff point. The value that generates the highest Youden index for a particular ratio is considered as the best cutoff for that ratio, as it provides highest discrimination between pathology and no pathology. The data are represented as mean ± standard deviation. A P-value of 0.05 or less was considered statistically significant.

Results

Patients and tumor characteristics

A total of 75 patients were enrolled in the present study, including 32 males (42.7%) and 43 females (57.3%), with a mean age of 38 ± 21.8 (range 26–66) years at the time of surgery. All the patients underwent a total thyroidectomy with or without neck dissection. Three patients underwent level II–VI lymph node dissection, 3 underwent level II and level III lymph node dissection, 5 underwent level II lymph node dissection, 3 underwent level IV and central lymph node dissection and 49 underwent central neck dissection. In addition, 12 patients underwent subtotal thyroidectomy without lymph node dissection. Among the 75 cases, 41 (54.6%) were diagnosed as PTC, 12 (16%) as FTC, 8 (10.6%) as MTC, 4 (5.3%) as ATC and 10 (13.3%) as simple goiter (Table 2). We also calculated the average miR-34a expression and considered 0.36 as the cutoff value. Expression lower than 0.36 was labeled as miR-34a-L and higher than 0.36 labeled as miR-34a-H. Among the 75 patients, miR-34a-L was identified in 41 cases (54.6%) and miR-34a-H in 34 cases (45.3%).

Association between miR-34a expression and clinicopathological features of thyroid carcinoma

As shown in Table 2, the miR-34a expression between I/II and III/IV changed significantly (0.41 ± 0.01 and 0.28 ± 0.02, respectively; $P < 0.001$). The mean expression of miR-34a in benign thyroid lesions (goiter) was 0.19 ± 0.01, while it was 0.38 ± 0.01 in thyroid carcinomas (PTC, FTC, MTC and ATC) ($P < 0.001$). In the malignant thyroid lesions, the miR-34a expression varied significantly among PTC, FTC, MTC and ATC with the mean value of 0.43 ± 0.08, 0.32 ± 0.04, 0.31 ± 0.05 and 0.27 ± 0.05, respectively ($P < 0.001$). As shown in Table 2 and Figure 2, the tumor stage, histopathology types and SUVmax demonstrated significant correlation with miR-34a expression (Table 2 and Figure 2).

FDG PET characteristics

All patients had SUVmax data for their primary thyroid lesions, and in patients with low (less than 3.63) and high SUVmax (equal to or more than 3.63), the mean expression of miR-34a was 0.43 ± 0.02 and 0.31 ± 0.01, respectively ($P = 0.0476$). There was a trend toward a lower normalized miR-34a expression in the primary tumor of patients with higher SUVmax than in patients with lower SUVmax ($P < 0.001$) (Table 2 and Figure 2D).
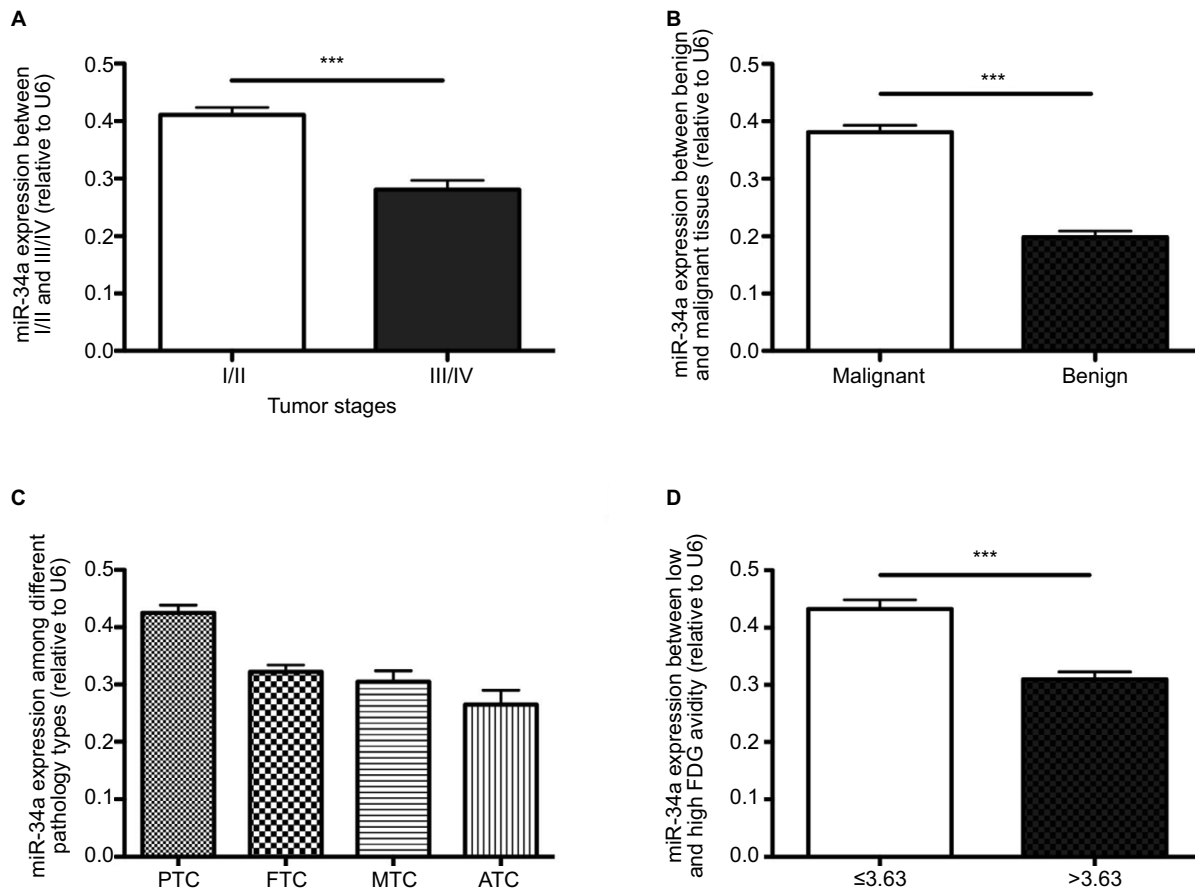
Figure 2 qRT-PCR results of miR-34a relative expression and the relationship between miR-34a expression and clinical characteristics in enrolled patients. Analysis of miR-34a relative expression by qRT-PCR. The results are shown as $2^{-\Delta\Delta Ct}$ and normalized to U6. There is no difference in the relative expression of miR-34a between patients of different ages and genders, with different lesion numbers and locations of lesions (data not shown). (**A**) Patients with higher tumor stage harbored lower miR-34a expression ($P < 0.001$), while (**B**) patients with malignant thyroid lesions expressed higher miR-34a than those with goiter ($P < 0.0001$). We also analyzed the miR-34a expression among different malignant pathology types and found that there is no significant difference among FTC, MTC and ATC. (**C**) However, tendency shows that ATC harbored lower miR-34a compared to other groups. (**D**) miR-34a expression was significantly higher in patients with low SUVmax (SUVmax ≤ 3.63) than in those with higher SUVmax (SUVmax >3.63, $P < 0.0001$). ***$P < 0.001$.

Abbreviations: FDG, fluorodeoxyglucose; FTC, follicular thyroid carcinoma; MTC, medullary thyroid carcinoma; ATC, anaplastic thyroid carcinoma; SUVmax, maximum standardized uptake value; PTC, papillary thyroid carcinoma.

ROC curves

The correlation between SUVmax and miR-34a expression was analyzed. An obvious negative correlation was observed with a Spearman correlation coefficient of –0.5528 ($P < 0.001$) (Figure 3A). ROC curve was generated using the logistic regression model for the normalized SUVmax of the primary tumor (Figure 4B); the area under the curve was 0.754. With an SUVmax of 4.3 as the threshold, sensitivity and specificity of the prediction of miR-34a expression were 70% and 94.3%, respectively. The area under the ROC curve was 0.843 (95% confidence interval [CI]: 0.749, 0.936; $P = 0.001$) (Figure 3B).

Inhibition of miR-34a expression upregulated GLUT1 expression in vitro

TPC-1 cells transfected with 45 nM miR-34a inhibitor or NC were cultured in full media. There was an approximately 55%

reduction of the miR-34a level in TPC-1 cells treated with the inhibitor (Figure 4A). As depicted in Figure 5B and C, both the mRNA and protein of GLUT1 were increased in TPC-1 cells treated with miR-34a inhibitor for 12 h. As expected, TPC-1 cells transfected with miR-34a inhibitor exhibited a significant upregulation of GLUT1 mRNA and protein (2.3-fold and 1.8-fold, respectively) compared with NC and control group ($P < 0.001$) (Figure 4B and C). Collectively, these results demonstrated that miR-34a could regulate the GLUT1 expression in TPC-1 cells.

Discussion

In the present study, we demonstrate that miR-34a is upregulated in malignant thyroid diseases and its expression is inversely associated with tumor stage and histopathology types. SUVmax can be used to predict miR-34a expression, and an inverse correlation between SUVmax and miR-34a
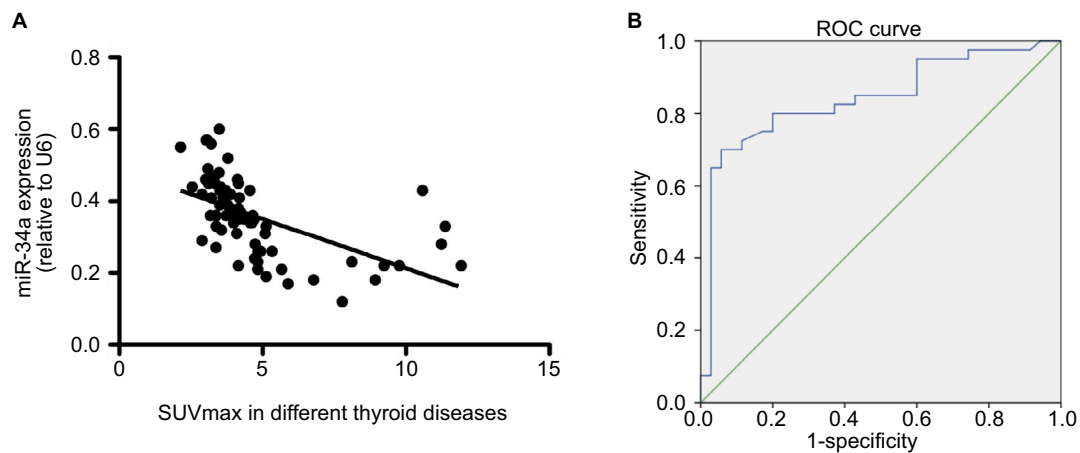
Figure 3 Graphs show the relationship between miR-34a expression and SUVmax in patients with thyroid diseases. (**A**) There was an inverse relationship between miR-34a expression and SUVmax in patients with thyroid diseases (Spearman correlation coefficient = –0.553, $P < 0.0001$). (**B**) ROC curve analysis of SUVmax to predict miR-34a expression. The miR-34a expression was divided into 2 different groups, named as miR-34a-L (whose miR-34a expression is lower than or equal to 0.36) and miR-34a-H (miR-34a expression is higher than 0.36). With an SUVmax of 4.3 as the threshold, sensitivity and specificity of the prediction of miR-34a expression (low or high) were 70% and 94.3%, respectively. The area under the ROC curve was 0.843 (95% confidence interval: 0.749, 0.936; $P = 0.001$).
Abbreviations: SUVmax, maximum standardized uptake value; ROC, receiver operating characteristic.
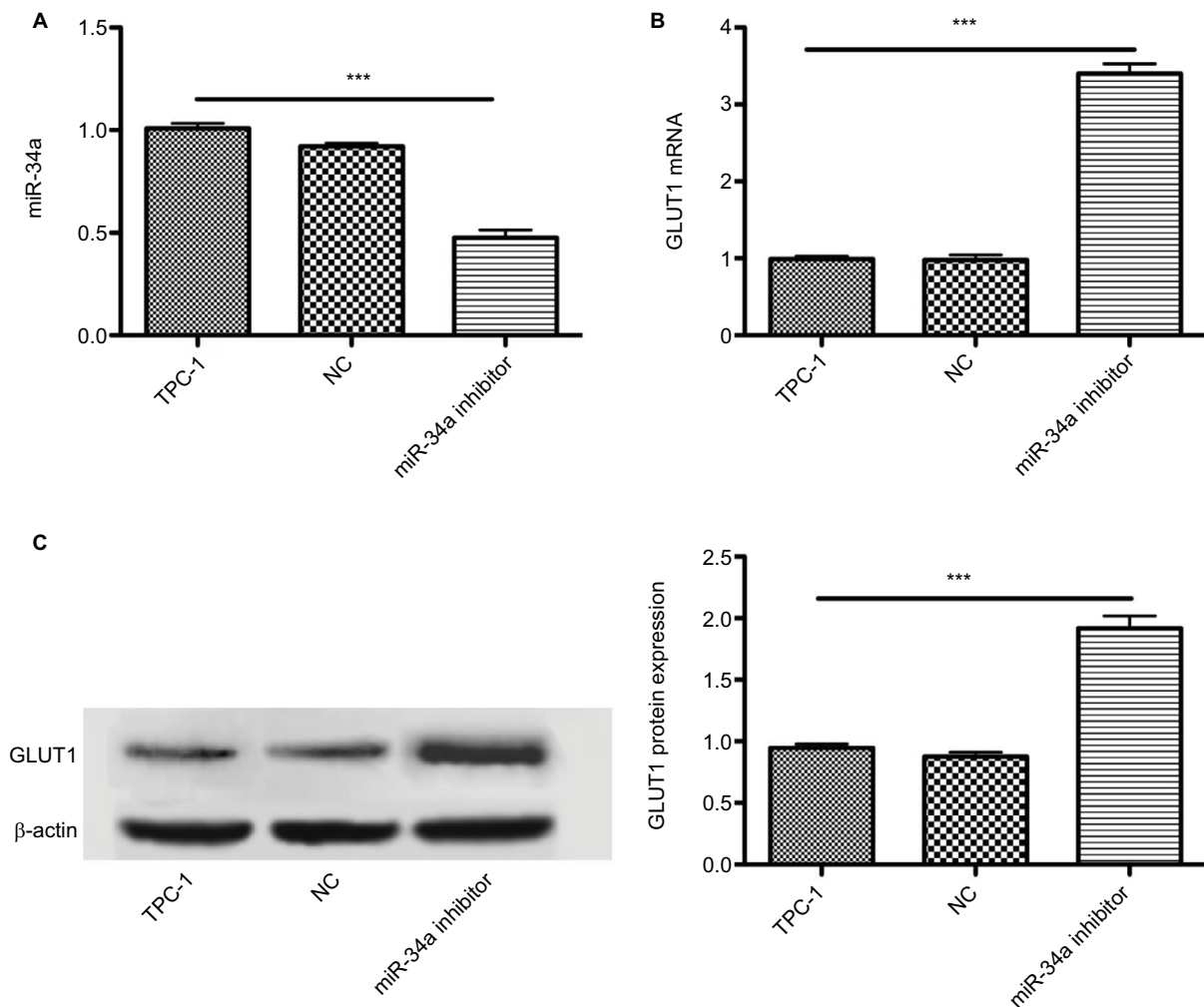

Figure 4 Inhibiting miR-34a expression increased GLUT1 expression. Graphs show the influence of miR-34 inhibition on glucose transporters in cultured TPC-1 cells. miR-34a may decrease ^{18}F-FDG uptake via targeting GLUT1 expression. Data are mean ± standard deviation. (**A**) miR-34a inhibitor successfully downregulated the miR-34a expression ($P < 0.001$), while there is no significant statistical difference between TPC-1 and NC group ($P > 0.05$). (**B** and **C**) Influence of miR-34a inhibition on expression of GLUT1 mRNA and protein in TPC-1 cells. miR-34a inhibition significantly increased expression of GLUT1 mRNA and protein (both $P < 0.001$). ***$P < 0.001$.
Abbreviations: GLUT1, glucose transporter 1; FDG, fluorodeoxyglucose; NC, negative control.
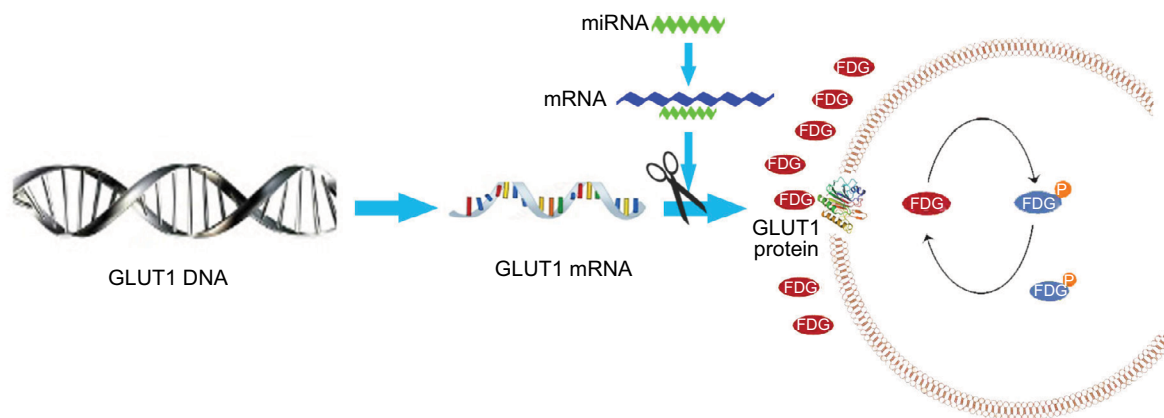
Figure 5 Models show the possible metabolic status in thyroid cancer with different miR-34a expression. miR-34a expression in ATC was lower than that in differentiated thyroid carcinoma, which cannot inhibit the GLUT1 expression, leading to increased FDG avidity. The glycolysis pathway, including ^{18}F-FDG uptake, was upregulated in patients with ATC. Thus, SUVmax was significantly higher in patients with ATC.
Abbreviations: ATC, anaplastic thyroid carcinoma; GLUT1, glucose transporter 1; FDG, fluorodeoxyglucose; SUVmax, maximum standardized uptake value; miRNA, microRNA.

expression was identified. With an SUVmax of 4.3 as the threshold, sensitivity and specificity of the prediction of miR-34a expression were 70% and 94.3%, respectively. The area under the ROC curve was 0.843 (95% CI: 0.749, 0.936; $P = 0.001$). We further inhibited the miR-34a expression in TPC-1 cells and both elevated GLUT1 mRNA and protein were detected, indicating that miR-34a possibly reduced the FDG avidity partially via targeting GLUT1 expression in thyroid cancers.

The incidence of thyroid disease has been increasing in the past decades throughout the world.[34–36] Microscopic nodules have been reported in approximately half of individuals, 3.5% have occult papillary carcinoma and 15% have palpable goiters.[37] Currently, the gold standard for thyroid nodule diagnosis is US-guided FNA biopsy, achieving correct final diagnoses in 70%–80% of cases; FNA biopsy is a reasonable approach to thyroid nodules for it has decreased costs substantially by facilitating selection of patients who need to undergo surgical excision.[38] However, the remaining 20%–30% of cases are considered indeterminate for malignancy.[39] Therefore, additional methods which can improve the sensitivity and specificity of diagnosis are highly desirable. Overcoming the challenges of accurate assessments of the risk for individual patients is important to establish appropriate treatment plans and optimize outcomes.

Numerous researches have shown that miRNAs play important roles in multiple biological and metabolic processes, including cell differentiation, proliferation, survival and malignancy.[8] miR-34 is a key regulator of tumor suppression. miR-34a, miR-34b and miR-34c are major members of the miR-34 precursor family. miR-34a is produced by its own transcript located in the second exon of chromosome 1, whereas miR-34b and miR-34c are produced by a common primary transcript derived from the second exon of chromosome 11.[40] Previous studies have shown that miR-34a was downregulated in a considerable number of cancers via repressing an assembly of genes promoting cell proliferation (Table 1). However, in contrast to its frequent decreased expression in numerous cancers, miR-34a has been found to be increased in thyroid carcinomas and cell lines.[41–43] In the present study, we confirmed that miR-34a is upregulated in malignant thyroid carcinoma, including PTC, FTC, MTC and ATC, compared with the benign tissues (Figure 2, $P < 0.001$). Importantly, although statistical difference is not significant, miR-34a expression was associated with the histopathology types and expressed lower in ATC, which is the most malignant among thyroid cancers, indicating that miR-34a may also play a tumor suppressor role in thyroid carcinoma. We not only confirmed the changes in miR-34a mRNA expression in thyroid cancers which was previously identified but also give insight into the different roles of miR-34a in thyroid cancer.[42] Ma et al revealed that overexpressing miR-34a promoted PTC cell proliferation and colony formation and inhibited apoptosis, whereas knockdown of miR-34a showed the opposite effects; furthermore, miR-34a overexpression led to activation of PI3K/Akt/Bad signaling pathway in PTC cells, and depletion of Akt reversed the pro-growth and antiapoptotic effects of miR-34a; thus, they concluded that miR-34a promotes proliferation and suppresses apoptosis in PTC cells via PI3K/Akt/Bad pathway, functioning as an oncogene in PTC.[25] However, we may not completely agree with their conclusions. First, they carried

out the study in TPC-1 cells, one of the human PTC cell lines. Although there were many common properties of the cell lines, each line had a unique profile of parameters, which most likely reflects the individuality of the tumors of origin and individual genotypes and capacity for a range of phenotypic expression of the cells.[44] Therefore, their conclusions may not represent the miR-34a function among other thyroid cell lines. Second, they carried out the experiment in TPC-1 cell line without analyzing the clinical significance of miR-34a in clinical samples, so possibly their study cannot reflect the virtual roles of miR-34a in clinical samples. In the present study, we analyzed the correlation between clinical characteristics and miR-34a expression based on clinical samples and confirmed that the tumor stage, histopathology types and SUVmax indeed influence the miR-34 expression. Moreover, our results demonstrated that tumors with high-level malignancy expressed lower miR-34a; elevated miR-34a in thyroid carcinoma, including PTC, FTC, MTC and ATC, may be an outcome of cells' reaction trying to protect themselves. Cong et al analyzed miRNA using 499 PTC samples and 58 normal thyroid tissues obtained from The Cancer Genome Atlas (TCGA) database and identified that miR-34a was upregulated in PTC tissues, which is consistent with our research.[45] Moreover, they revealed that miR-34a expression was higher in later tumor stage (2.69 in III/IV stage vs. 2.61 in I/II stage, $P = 0.004$), which seems different from our study. This disparity may be caused on the one hand by the different patient cohorts (PTC only in Cong et al's study, while PTC, FTC, MTC and ATC in the current study); on the other hand, Cong's research included different patients of different regions, ages, races and so on, so possibly heterogeneity within the group is inevitable. Fritz et al conformed that miR-34a function as a tumor suppressor in renal cell carcinoma (RCC) whereas they found miR-34a to be upregulated in a larger cohort of RCC patients,[22] indicating that tumor suppressor does not have to be downregulated. Although Dalgard et al confirmed tumor suppressor activity for miR-34a, they also observed differential levels of miR-34a expression in different retinal blastoma cells and clinical sample tissues.[46] Moreover, differential miR-34a expression is also observed in breast, melanoma, pancreatic and prostate cancer cell lines.[47] These phenomena can be explained by gain or loss of 1p36 at the miR-34a loci, CpG methylation silencing or genomic alteration at the p53-binding site in the miR-34a gene. In the present study, no significant correlations were identified between miR-34a expression and other clinicopathological features of thyroid diseases, including age, gender, lesion numbers and the position of lesions.

^{18}F-FDG uptake is based on enhanced aerobic glycolysis in cancer cells, known as Warburg effect.[48] Several investigators have shown that FDG positive avidity is likely to be associated with a larger tumor size, the presence of extrathyroid extension and lymph node metastasis in patients with PTC;[49] however, others have declared that there is no correlation between the SUVmax in primary PTC and the presence of multifocality, extrathyroid extension of primary PTC or lymph node metastasis.[50] As miR-34a could serve as a therapeutic target, using miR-34a mimics may lead to restoration of the level of miR-34a and many target proteins, and thus to an improvement of the disease. miR-based treatment is currently becoming a reality as there are many biotech companies focusing on the use of miRNAs. Using SUVmax to predict the miRNA expression is safe and nonintrusive. In the current study, we demonstrated that there is an obvious correlation between SUVmax and miR-34a expression, and with a cutoff value of 4.3, SUVmax can effectively predict the miRNA expression (Figure 3).

Previous studies have shown that there was significant correlation between the expression of GLUT1 and SUVmax in ^{18}F-FDG PET/CT, indicating that GLUT1 plays an important role in increasing FDG uptake.[51,52] To explore the potential mechanisms by which miR-34a regulates FDG avidity, we carried out other experiments in TPC-1 cells. After inhibiting the miR-34a, we detected the GLUT1 expression and found increased GLUT1 mRNA and protein (Figure 4), indicating that miR-34a possibly inhibits FDG avidity by targeting GLUT1 in thyroid cancers (Figure 5).

Our study has several unique strengths. First, this single-center study on thyroid lesions limits participant heterogeneity and variations in tumor subtypes. Second, our finding that the miR-34a expression was associated with clinicopathological parameters suggests the utility of preoperative miR-34a analysis in risk stratification and surgical management. Lastly, we analyzed the relationship between miR-34a expression and ^{18}F-FDG PET/CT features in both malignant thyroid carcinoma and benign lesions and found out that the SUVmax can ideally be used to predict the miR-34a expression.

Some limitations in our study need to be declared. First, the sample size (75 patients) was relatively small and this is partially due to the strict inclusion criteria (primary diagnosis, untreated and complete pathology results). Second, the current study was conducted at one hospital, which means the present results are relatively limited. Third, this was a retrospective study, and there was unavoidable selection bias. Further large prospective studies that include more hospitals and clinical samples are urgently needed to consolidate our

results. Finally, the interaction between miR-34a and GLUT1 is indirect and more substantial evidence should be digged out. In addition, more specific experiments illustrating the interaction between miR-34a and GLUT1 (luciferase reporter essay, for example) should be carried out.

Conclusion

Collectively, we found that in patients with malignant thyroid lesions, miR-34a expression is upregulated compared with the benign tumors or goiters and associated with tumor stage and histopathology types; moreover, an inverse correlation between ^{18}F-FDG PET/CT avidity was confirmed and miR-34a may regulate FDG uptake partially via targeting GLUT1, which needs to be validated in our future study.

Acknowledgments

Disclosure

The authors report no conflict of interest in this work.

References

1. Carneiro RM, Carneiro BA, Agulnik M, Kopp PA, Giles FJ. Targeted therapies in advanced differentiated thyroid cancer. *Cancer Treat Rev*. 2015;41(8):690–698.
2. Vucemilo L, Znaor T, Kulis T, Sekerija M, Znaor A. Thyroid cancer incidence and mortality trends in Croatia 1988-2010. *Acta Clin Croat*. 2015;54(1):30–37.
3. Morris LG, Sikora AG, Tosteson TD, Davies L. The increasing incidence of thyroid cancer: the influence of access to care. *Thyroid*. 2013;23(7):885–891.
4. Veiga LH, Neta G, Aschebrook-Kilfoy B, Ron E, Devesa SS. Thyroid cancer incidence patterns in Sao Paulo, Brazil, and the U.S. SEER program, 1997-2008. *Thyroid*. 2013;23(6):748–757.
5. Mitro SD, Rozek LS, Vatanasapt P, et al. Iodine deficiency and thyroid cancer trends in three regions of Thailand, 1990-2009. *Cancer Epidemiol*. 2016;43(8):92–99.
6. Zheng X, Wei S, Han Y, et al. Papillary microcarcinoma of the thyroid: clinical characteristics and BRAF(V600E) mutational status of 977 cases. *Ann Surg Oncol*. 2013;20(7):2266–2273.
7. Lee MJ, Hong SW, Chung WY, Kwak JY, Kim MJ, Kim EK. Cytological results of ultrasound-guided fine-needle aspiration cytology for thyroid nodules: emphasis on correlation with sonographic findings. *Yonsei Med J*. 2011;52(5):838–844.
8. Alvarez-Garcia I, Miska EA. MicroRNA functions in animal development and human disease. *Development*. 2005;132(21):4653–4662.
9. Maroni P, Puglisi R, Mattia G, et al. In bone metastasis miR-34a-5p absence inversely correlates with Met expression, while Met oncogene is unaffected by miR-34a-5p in non-metastatic and metastatic breast carcinomas. *Carcinogenesis*. 2017;38(5):492–503.
10. Wang Y, Chen J, Chen X, et al. MiR-34a suppresses HNSCC growth through modulating cell cycle arrest and senescence. *Neoplasma*. 2017;64(4):543–553.
11. Zhou Y, Huang T, Siu HL, et al. IGF2BP3 functions as a potential oncogene and is a crucial target of miR-34a in gastric carcinogenesis. *Mol Cancer*. 2017;16(1):77.
12. Pu Y, Zhao F, Wang H, Cai S. MiR-34a-5p promotes multi-chemoresistance of osteosarcoma through down-regulation of the DLL1 gene. *Sci Rep*. 2017;7(3):44218.
13. Yan K, Gao J, Yang T, et al. MicroRNA-34a inhibits the proliferation and metastasis of osteosarcoma cells both in vitro and in vivo. *PLoS One*. 2012;7(3):e33778.
14. Di Martino MT, Leone E, Amodio N, et al. Synthetic miR-34a mimics as a novel therapeutic agent for multiple myeloma: in vitro and in vivo evidence. *Clin Cancer Res*. 2012;18(22):6260–6270.
15. Cai H, Zhou H, Miao Y, Li N, Zhao L, Jia L. MiRNA expression profiles reveal the involvement of miR-26a, miR-548l and miR-34a in hepatocellular carcinoma progression through regulation of ST3GAL5. *Lab Invest*. 2017;97(5):530–542.
16. Sun TY, Xie HJ, Li Z, et al. miR-34a regulates HDAC1 expression to affect the proliferation and apoptosis of hepatocellular carcinoma. *Am J Trans Res*. 2017;9(1):103–114.
17. Pramanik D, Campbell NR, Karikari C, et al. Restitution of tumor suppressor microRNAs using a systemic nanovector inhibits pancreatic cancer growth in mice. *Mol Cancer Ther*. 2011;10(8):1470–1480.
18. Yamazaki H, Chijiwa T, Inoue Y, et al. Overexpression of the miR-34 family suppresses invasive growth of malignant melanoma with the wild-type p53 gene. *Exp Ther Med*. 2012;3(5):793–796.
19. Sun C, Wang FJ, Zhang HG, et al. miR-34a mediates oxaliplatin resistance of colorectal cancer cells by inhibiting macroautophagy via transforming growth factor-beta/Smad4 pathway. *World J Gastroenterol*. 2017;23(10):1816–1827.
20. Daugaard I, Knudsen A, Kjeldsen TE, Hager H, Hansen LL. The association between miR-34 dysregulation and distant metastases formation in lung adenocarcinoma. *Exp Mol Pathol*. 2017;102(3):484–491.
21. Liu L, Ren W, Chen K. MiR-34a promotes apoptosis and inhibits autophagy by targeting HMGB1 in acute myeloid leukemia cells. *Cell Physiol Biochem*. 2017;41(5):1981–1992.
22. Fritz HK, Gustafsson A, Ljungberg B, Ceder Y, Axelson H, Dahlback B. The Axl-regulating tumor suppressor miR-34a is increased in ccRCC but does not correlate with Axl mRNA or Axl protein levels. *PLoS One*. 2015;10(8):e0135991.
23. Chandrasekaran KS, Sathyanarayanan A, Karunagaran D. Downregulation of HMGB1 by miR-34a is sufficient to suppress proliferation, migration and invasion of human cervical and colorectal cancer cells. *Tumour Biol*. 2016;37(10):13155–13166.
24. Wen D, Peng Y, Lin F, Singh RK, Mahato RI. Micellar delivery of miR-34a modulator rubone and paclitaxel in resistant prostate cancer. *Cancer Res*. 2017;77(12):3244–3254.
25. Ma Y, Qin H, Cui Y. MiR-34a targets GAS1 to promote cell proliferation and inhibit apoptosis in papillary thyroid carcinoma via PI3K/Akt/Bad pathway. *Biochem Biophys Res Commun*. 2013;441(4):958–963.
26. Lu X, Chen Z, Liang H, et al. Thyroid hormone inhibits TGFbeta1 induced renal tubular epithelial to mesenchymal transition by increasing miR34a expression. *Cell Signal*. 2013;25(10):1949–1954.
27. Sachpekidis C, Dettmer MS, Weidner S, Giger R, Wartenberg J. 18F-FDG PET/CT of papillary carcinoma in a lateral thyroglossal duct cyst. *Clin Nucl Med*. 2017;42(8):e371–e374.
28. Vera P, Edet-Sanson A, Quieffin F, et al. Diffusion-weighted MRI is not superior to FDG-PET/CT for the detection of neck recurrence in well-differentiated thyroid carcinoma. *Q J Nucl Med Mol Imaging*. 2017;3(3).
29. Choi EK, Chong A, Ha JM, Jung CK, O JH, Kim SH. Clinicopathological characteristics including BRAF V600E mutation status and PET/CT findings in papillary thyroid carcinoma. *Clin Endocrinol*. 2017;87(1):73–79.
30. Kong L, Zhu J, Han W, et al. Significance of serum microRNAs in pre-diabetes and newly diagnosed type 2 diabetes: a clinical study. *Acta Diabetol*. 2011;48(1):61–69.
31. Nagarajan A, Dogra SK, Sun L, et al. Paraoxonase 2 facilitates pancreatic cancer growth and metastasis by stimulating GLUT1-mediated glucose transport. *Mol Cell*. 2017;67(4):685.e6–701.e6.
32. Wang J, Ye C, Chen C, et al. Glucose transporter GLUT1 expression and clinical outcome in solid tumors: a systematic review and meta-analysis. *Oncotarget*. 2017;8(10):16875–16886.

33. Amin MB, Greene FL, Edge SB, et al. The Eighth Edition AJCC Cancer Staging Manual: continuing to build a bridge from a population-based to a more "personalized" approach to cancer staging. *CA Cancer J Clin.* 2017;67(2):93–99.

34. Shah BR, Griffiths R, Hall SF. Thyroid cancer incidence among Asian immigrants to Ontario, Canada: a population-based cohort study. *Cancer.* 2017;123(17):3320–3325.

35. Fallahi P, Ferrari SM, Ruffilli I, et al. Incidence of thyroid disorders in mixed cryoglobulinemia: results from a longitudinal follow-up. *Autoimmunity Rev.* 2016;15(7):747–751.

36. O'Grady TJ, Gates MA, Boscoe FP. Thyroid cancer incidence attributable to overdiagnosis in the United States 1981-2011. *Int J Cancer.* 2015;137(11):2664–2673.

37. La Vecchia C, Malvezzi M, Bosetti C, et al. Thyroid cancer mortality and incidence: a global overview. *Int J Cancer.* 2015;136(9): 2187–2195.

38. Gharib H. Fine-needle aspiration biopsy of thyroid nodules: advantages, limitations, and effect. *Mayo Clin Proc.* 1994;69(1):44–49.

39. Rumyantsev PO, Saenko VA, Ilyin AA, et al. Radiation exposure does not significantly contribute to the risk of recurrence of Chernobyl thyroid cancer. *J Clin Endocrinol Metab.* 2011;96(2):385–393.

40. Misso G, Di Martino MT, De Rosa G, et al. Mir-34: a new weapon against cancer? *Mol Ther Nucl Acids.* 2014;3:e194.

41. Cahill S, Smyth P, Finn SP, et al. Effect of ret/PTC 1 rearrangement on transcription and post-transcriptional regulation in a papillary thyroid carcinoma model. *Mol Cancer.* 2006;5:70.

42. Sheu SY, Grabellus F, Schwertheim S, Worm K, Broecker-Preuss M, Schmid KW. Differential miRNA expression profiles in variants of papillary thyroid carcinoma and encapsulated follicular thyroid tumours. *Br J Cancer.* 2010;102(2):376–382.

43. Yang L-J, Wang D-G, Chen J-Y, Zhang H-Y, Zhang F-F, Mou Y-H. Expression of miR-34a and its role in human papillary thyroid carcinoma. *Int J Clin Exp Pathol.* 2017;10(3):3258–3264.

44. Bigner DD, Bigner SH, Ponten J, et al. Heterogeneity of genotypic and phenotypic characteristics of fifteen permanent cell lines derived from human gliomas. *J Neuropathol Exp Neurol.* 1981;40(3):201–229.

45. Cong D, He M, Chen S, Liu X, Liu X, Sun H. Expression profiles of pivotal microRNAs and targets in thyroid papillary carcinoma: an analysis of The Cancer Genome Atlas. *Onco Targets Ther.* 2015;8:2271–2277.

46. Dalgard CL, Gonzalez M, deNiro JE, O'Brien JM. Differential microRNA-34a expression and tumor suppressor function in retinoblastoma cells. *Invest Ophthalmol Visual Sci.* 2009;50(10):4542–4551.

47. Lodygin D, Tarasov V, Epanchintsev A, et al. Inactivation of miR-34a by aberrant CpG methylation in multiple types of cancer. *Cell Cycle.* 2008;7(16):2591–2600.

48. American Academy of Pediatrics. On the origin of cancer cells. *Pediatrics.* 1956;17(5):746.

49. Yun M, Noh T-W, Cho A, et al. Visually discernible [18F] fluorodeoxyglucose uptake in papillary thyroid microcarcinoma: a potential new risk factor. *J Clin Endocrinol Metab.* 2010;95(7):3182–3188.

50. Jeong HS, Chung M, Baek CH, Ko YH, Choi JY, Son YI. Can [18F] – fluorodeoxyglucose standardized uptake values of PET imaging predict pathologic extrathyroid invasion of thyroid papillary microcarcinomas? *Laryngoscope.* 2006;116(12):2133–2137.

51. Horiuchi C, Tsukuda M, Taguchi T, Ishiguro Y, Okudera K, Inoue T. Correlation between FDG-PET findings and GLUT1 expression in salivary gland pleomorphic adenomas. *Ann Nucl Med.* 2008;22(8):693–698.

52. Wang ZG, Yu MM, Han Y, et al. Correlation of Glut-1 and Glut-3 expression with F-18 FDG uptake in pulmonary inflammatory lesions. *Medicine (Baltimore).* 2016;95(48):e5462.